

# Direct dark matter search by observing electrons produced in neutralino-nucleus collisions

Ch. C. Moustakidis<sup>1\*</sup>, J. D. Vergados<sup>2†</sup>, and H. Ejiri<sup>3‡</sup>

<sup>1</sup>*Department of Theoretical Physics,  
Aristotle University of Thessaloniki,  
54124 Thessaloniki Greece*

<sup>2</sup>*University of Ioannina, 45110 Ioannina, Greece*

<sup>3</sup>*NS, International Christian University,  
Osawa, Mitaka, Tokyo, 181-8585, Japan*

## Abstract

Exotic dark matter and dark energy together seem to dominate in the Universe. Supersymmetry naturally provides a candidate for the dark matter constituents via the lightest supersymmetric particle (LSP). The most important process for directly detecting dark matter is the LSP-nucleus elastic scattering by measuring the energy of the recoiling nucleus. In the present work we explore a novel process, which has definite experimental advantages, that is the detection of the dark matter constituents by observing the low energy ionization electrons. These electrons, which are produced during the LSP-nucleus collision, may be observed separately or in coincidence with the recoiling nuclei. We develop the formalism and apply it in calculating the ratio of the ionization rate to the nuclear recoil rate in a variety of atoms including <sup>20</sup>Ne, <sup>40</sup>Ar, <sup>76</sup>Ge, <sup>78</sup>Kr and <sup>132</sup>Xe employing realistic Hartree-Fock

---

\*e-mail: moustaki@auth.gr

†e-mail: Vergados@cc.uoi.gr

‡e-mail: ejiri@rcnp.osaka-u.ac.jp

electron wave functions. The obtained ratios are essentially independent of all parameters of supersymmetry except the neutralino mass, but they crucially depend on the electron energy cut off. These ratios per electron tend to increase with the atomic number and can be as high as 10%. Based on our results it is both interesting and realistic to detect the LSP by measuring the ionization electrons following the-LSP nuclear collisions.

Keywords: LSP, Direct neutralino search, ionization electrons, electron detection, dark matter, WIMP.

PACS : 95.35+d, 12.60.Jv.

## 1 Introduction

From the rotational curves of objects outside the luminous galaxies it has been known for some time that there must be dark (non luminous) matter in the Universe. Furthermore the combined MAXIMA-1 [1], BOOMERANG [2], DASI [3] and COBE/DMR [4] Cosmic Microwave Background (CMB) observations as well as the high precision recent WMAP data [5]-[6] imply that the Universe is flat [7] and it is dominated by dark matter and dark energy (cosmological constant). Crudely speaking one has:

$$\Omega_b = 0.05, \quad \Omega_{CDM} = 0.30, \quad \Omega_\Lambda = 0.65$$

for the baryonic, dark matter and dark energy fractions, respectively. It is also known that the non exotic component cannot exceed 40% of the CDM [8]. So there is plenty of room for the exotic WIMPs (Weakly Interacting Massive Particles).

Many experiments are currently under way aiming at the direct detection of WIMPs. In fact the DAMA experiment [9] has claimed the observation of such events, which with better statistics have subsequently been interpreted as a modulation signal [10]. These data, however, if interpreted as due to the scalar interaction, are not consistent with other recent experiments, see e.g. EDELWEISS [11] and CDMS [12].

Supersymmetry naturally provides candidates for the dark matter constituents [13],[14]-[17]. In the most favored scenario of supersymmetry the

lightest supersymmetric particle (LSP) can be simply described as a Majorana fermion, a linear combination of the neutral components of the gauginos and higgsinos [13],[14]-[24].

The event rates, however, are expected to be quite low and the nuclear recoil energies are extremely small. Thus one has to try to reduce the background to the lowest possible level and to understand possible origins of backgrounds to be corrected for [25]. Anyway one has to search for characteristic signatures associated with the LSP. Such are:

- The time dependence of the event rates, which is due to the motion of the Earth (modulation effect). Unfortunately, however, the modulation effect is small,  $\leq 2\%$ , and for heavy targets the relevant sign depends on the LSP mass. So one cannot accurately predict even when the maximum occurs. Furthermore one should keep in mind that there are seasonal effects on the background as well.
- The correlation of the observed rates of directionally sensitive experiments with the motion of the sun [26, 27, 28]. In this case one has large asymmetries and larger relative modulation amplitudes, with characteristic directional dependence. These are, indeed, very interesting signatures, but the expected event rates are suppressed by a factor of at least  $4\pi$  relative to the standard rates. Furthermore, at present, the experiments are able to measure the direction of nuclear recoil, but it will be extremely difficult to determine the sense of direction [29].
- Inelastic excitations to low lying excited nuclear states have also been considered [30, 31]. In this case one can overcome the difficulties encountered in the recoil experiments (energy threshold, quenching factors etc) by detecting the de-excitation  $\gamma$ -rays. The predicted branching ratios, due to the spin induced DM cross sections, in favorable circumstances can be as high as 10%, which is a very encouraging result.
- Detecting the dark matter constituents by observing the low energy electrons, which follow the ionization of the atom during the LSP-nucleus collision [25].

The last possibility may be realized with the technology of gaseous TPC detectors [32]-[34]. In fact the WIMP-nucleus scattering leads: (i) to nuclear recoil without atomic excitations and (ii) to nuclear recoil with atomic excitations. So far most CDM searches have been made by the inclusive processes,

(i) and (ii), employing solid detectors. We propose that the produced electrons in atomic excitation (ii) should be studied by exclusive measurements. In a previous calculation [25] we have estimated the ratio of the ionization rate (per electron) by considering the simple target  $^{20}\text{Ne}$  assuming hydrogenic electron wave functions.

In the present paper we extend these calculations by considering a number of experimentally interesting targets. To this end realistic Hartree-Fock electron wave functions have been employed. The observed ratio of the electron rate (ii) for one electron per atom, to be denoted below as per electron, divided by the standard nuclear recoil rate (i), depends, of course, on the low energy cut off for both electrons (tenths of keV) and nuclear recoils (10-20 keV) as well as the quenching factor for recoils. They can reach It is found to increase as the atomic number and it can get as high as 10% for a reasonable choice of these parameters. The experimentally interesting quantity the ratio per atom, meaning that one considers all electrons in the atom, obtained from the previous one by multiplying it with  $Z$ . This ratio for medium and heavy nuclei may even become larger than unity. Thus this method can be widely used for any target nuclei with adequate electron detection capability. The present paper is organized as follows: The theoretical framework is presented in Sec. 2, the main results are shown in Sec. 3 and a brief summary is given in Sec. 4.

## 2 The essential ingredients of our calculation

The electron ionization due to the LSP collisions can take place via two mechanisms:

1. The electrons are ejected during the LSP-nucleus collisions via the standard EM interactions.
2. The electrons are ejected due to the LSP-electron interaction. This interaction is obtained in a fashion analogous to the LSP-quark interaction. In the case of the  $Z$  and Higgs exchange one replaces the relevant quark couplings [35] by the electron couplings. In the s-fermion mediated mechanism the s-quarks are replaced by s-electrons. In fact this mechanism has recently been proposed as providing a possibility of LSP detection in electron accelerators [36]. In the present case, however, one can get reasonably high electron energies, of a few hundreds

of electron volts, only if one exploits electrons bound in nuclei. Then the kinematics is similar to that of the previous mechanism.

Since the branching ratios of the second case depend on the SUSY parameter space and one does not enjoy the effect of coherence arising from the scalar interaction, we will concentrate here in the first mechanism.

## 2.1 The formalism

The differential cross section for the LSP nucleus scattering leading to the emission of electrons in the case of non-relativistic neutralino takes the form [25]

$$d\sigma(\mathbf{k}) = \frac{1}{v} \frac{m_e}{E_e} |M|^2 \frac{d\mathbf{q}}{(2\pi)^3} \frac{d\mathbf{k}}{(2\pi)^3} (2\pi)^3 \frac{1}{2(2l+1)} \sum_{nlm} p_{nl} \times \quad (1)$$

$$\left[ \tilde{\phi}_{nlm}(\mathbf{k}) \right]^2 2\pi \delta \left( T_\chi + \epsilon_{nl} - T - \frac{q^2}{2m_A} - \frac{(\mathbf{p}_\chi - \mathbf{k} - \mathbf{q})^2}{2m_\chi} \right)$$

where  $v$ ,  $T_\chi$  and  $\mathbf{p}_\chi$  are the oncoming LSP velocity, energy and momentum distribution, while  $\mathbf{q}$  is the momentum transferred to the nucleus.  $M$  is the invariant amplitude, known from the standard neutralino nucleus cross section,  $T$  and  $\mathbf{k}$  are the kinetic energy and the momentum of the outgoing electron and  $\epsilon_{nl}$  is the energy of the initial electron, which is, of course, negative.  $\tilde{\phi}_{nlm}(\mathbf{k})$  is the Fourier transform of the bound electron wave function, i.e., its wave function in momentum space.  $p_{nl}$  is the probability of finding the electron in the  $n, l$  orbit. In the expression above and in what follows our normalization will consist of one electron per atom, to be compared with the cross section per nucleus of the standard experiments.

In order to avoid any complications arising from questions regarding the allowed SUSY parameter space, we will present our results normalized to the standard neutralino-nucleus cross section. The obtained branching ratios are essentially independent of all parameters of supersymmetry except the neutralino mass.

With these ingredients we find that the ratio of the cross section with ionization divided by that of the standard neutralino-nucleus elastic scattering, nuclear recoil experiments (nrec), takes the form

$$\frac{d\sigma(T)}{\sigma_{nrec}} = \frac{1}{4} \sum_{nl} p_{nl} |\tilde{\phi}_{nl}(\sqrt{2m_e T})|^2 m_e \sqrt{2m_e T}$$

$$\times \frac{\int_{-1}^1 d\xi_1 \int_{\xi_L}^1 d\xi K \frac{(\xi+\Lambda)^2}{\Lambda} [F(\mu_r v(\xi + \Lambda))]^2}{\int_0^1 2\xi d\xi [F(2m_r v\xi)]^2} dT \quad (2)$$

where  $\mu_r$  the LSP-nucleus reduced mass and also

$$\begin{aligned} \Lambda &= \sqrt{\xi^2 - \xi_L^2} \\ \xi_L &= \sqrt{\frac{m_\chi}{\mu_r} \left[ 1 + \frac{1}{K^2} \left( \frac{T - \epsilon_{nl}}{T_\chi} - 1 \right) \right]} \end{aligned} \quad (3)$$

with

$$\begin{aligned} \mathbf{K} &= \frac{\mathbf{p}_\chi - \mathbf{k}}{p_\chi}, \quad K = \frac{\sqrt{p_\chi^2 + k^2 - 2kp_\chi\xi_1}}{p_\chi} \\ \xi_1 &= \hat{p}_\chi \cdot \hat{k}, \quad \xi = \hat{q} \cdot \hat{K} \end{aligned} \quad (4)$$

$2\frac{\mu_r}{m_\chi}p_\chi\xi = 2\mu_r v\xi$  is the momentum  $q$  transferred to the nucleus and  $F(q)$  is the nuclear form factor. For a given LSP energy, the outgoing electron energy lies in the range given by:

$$0 \leq T \leq \frac{\mu_r}{m_\chi}T_\chi + \epsilon_{nl}. \quad (5)$$

Since the momentum of the outgoing electron is much smaller than the momentum of the oncoming neutralino, i.e.,  $K \approx 1$ , the integration over  $\xi_1$  can be trivially performed. Furthermore, if the effect of the nuclear form factor can be neglected, the integration over  $\xi$  can be performed analytically. Thus we get

$$\begin{aligned} \frac{d\sigma(T)}{\sigma_{nrec}} &= \frac{1}{2} \sum_{nl} p_{nl} |\tilde{\phi}_{nl}(\sqrt{2m_e T})|^2 m_e \sqrt{2m_e T} \times \\ &\left[ 1 - \left( \frac{m_\chi (T - \epsilon_{nl})}{\mu_r T_\chi} \right) + \sqrt{1 - \left( \frac{m_\chi (T - \epsilon_{nl})}{\mu_r T_\chi} \right)} \right] dT \end{aligned} \quad (6)$$

Otherwise the angular integrations can only be done numerically. Finally one must integrate numerically the above expression over the electron spectrum to obtain the total cross section as a function of the neutralino energy (velocity). The folding with the LSP velocity will be done at the level of the event rates (see sec. 2.4)

## 2.2 The role of the nuclear form factor

The nuclear form factor  $F(u)$  entering in Eq. (2) has the general form

$$F(u) = \frac{Z}{A}F_Z(u) + \frac{N}{A}F_N(u) \quad (7)$$

The proton and neutron form factors ( $F_Z(u)$  and  $F_N(u)$  respectively) are calculated by the Fourier transform of the proton density distribution  $\rho_Z(\mathbf{r})$  and neutron density distribution  $\rho_N(\mathbf{r})$  respectively. In the present work  $\rho_Z(\mathbf{r})$  and  $\rho_N(\mathbf{r})$  are constructed using harmonic oscillator wave functions. More specifically the densities are defined as

$$\rho_{Z,N}(\mathbf{r}) = \sum_i \phi_i^*(\mathbf{r})\phi_i(\mathbf{r}) \quad (8)$$

where the sum run all over the proton ( neutron) orbitals  $\phi_i(\mathbf{r})$ . In general some of the nuclei considered in this work may be deformed. Thus, strictly speaking, the densities depend not only on the radial coordinate  $r$  but on the angle  $\theta$  as well. In the present work, however, we are mainly interested in branching ratios, which depend very little on the nuclear form factor. Thus to a good approximation the nuclei can be treated as spherical. Thus in the case of the heaviest nuclear system considered in this work, namely  $^{132}\text{Xe}$ , for a threshold energy of  $E_{th} = 0.2$  keV the effect of the form factor is a reduction of the branching ratio by less than 7%. For this reason we have included only one stable isotope, namely the most abundant one, which is indicated on the figures.

In view of the above the form factor is given by the relation:

$$F_{Z,N}(q) = \int e^{i\mathbf{q}\mathbf{r}}\rho_{Z,N}(r)d\mathbf{r} \quad (9)$$

The nuclear form factor of  $^{20}\text{Ne}$  is taken from Ref. [37], where the nuclear wave functions were obtained by shell model calculations using the Wildenthal interaction. The nuclear form factors of the heavier nuclei were for simplicity calculated by using spherical harmonic oscillator wave functions. This is a good approximation since, as it has already been mentioned, the ratio of the two processes we is insensitive to the details of the nuclear wave functions.

### 2.3 The bound electron wave functions

In the present work we consider very accurate spin-independent atomic wave functions obtained by Bunge *et al* [38], by applying the Roothaan-Hartree-Fock method (RHF) to calculate analytical self-consistent-field atomic wave function. In principle one should employ the relativistic electron wave functions, especially for the inner shell electrons of large  $Z$  atoms. Anyway for our purposes the above wave functions are adequate, since the inner shell electrons contribute only a small fraction to the rate. In this approach the radial atomic orbitals  $R_{n\ell}$  are expanded as a finite superposition of primitive radial functions

$$R_{n\ell}(r) = \sum_j C_{jn\ell} S_{j\ell}(r) \quad (10)$$

where the normalized primitive basis  $S_{j\ell}(r)$  is taken as a Slater-type orbital set,

$$S_{j\ell}(r) = N_{j\ell} r^{n_{j\ell}-1} e^{-Z_{j\ell} r} \quad (11)$$

where the normalization factor  $N_{j\ell}$  is given by

$$N_{j\ell} = (2Z_{j\ell})^{(n_{j\ell}+1/2)} / [(2n_{j\ell})!]^{1/2} \quad (12)$$

and  $n_{j\ell}$  is the principal quantum number,  $Z_{j\ell}$  is the orbital exponent, and  $\ell$  is the azimuthal quantum number.

The atomic wave functions in the momentum space are related to the coordinate wave functions by

$$\tilde{\phi}_{n\ell m}(\mathbf{k}) = \frac{1}{(2\pi)^{3/2}} \int e^{-i\mathbf{k}\mathbf{r}} \phi_{n\ell m}(\mathbf{r}) d\mathbf{r} \quad (13)$$

where  $n\ell m$  denote the usual quantum numbers characterizing atomic states. The radial momentum-wave function defined as

$$\tilde{\phi}_{n\ell m}(\mathbf{k}) = (-i)^\ell \tilde{R}_{n\ell}(k) Y_{\ell m}(\Omega_k) \quad (14)$$

is related to the radial wave function in coordinate space through (see also [39])

$$\tilde{R}_{n\ell}(k) = \sqrt{\frac{2}{\pi}} \int_0^\infty r^2 R_{n\ell}(r) j_\ell(kr) dr \quad (15)$$

where  $j_\ell(kr)$  is a spherical Bessel function. The radial wave functions in momentum space  $\tilde{R}_{n\ell}(k)$  are written as

$$\tilde{R}_{n\ell}(k) = \sum_j C_{jn\ell} \tilde{S}_{j\ell}(k) \quad (16)$$



in term of the RHF functions  $\tilde{S}_{j\ell}(k)$  in momentum space, related to  $S_{j\ell}(r)$  through

$$\tilde{S}_{j\ell}(k) = \sqrt{\frac{2}{\pi}} \int_0^\infty r^2 S_{j\ell}(r) j_\ell(kr) dr \quad (17)$$

The needed binding energies were taken from [40].

## 2.4 Folding with the LSP velocity distribution

The above results were derived assuming a definite LSP velocity. In practice, however, the LSP obeys a velocity distribution. The actual velocity distribution may be complicated, i.e. asymmetric and varying from one point to another. In our vicinity it is commonly assumed that LSP obeys a simple Maxwell-Boltzmann velocity distribution with respect to the galactic center [28], namely

$$f(v) = \frac{1}{(v_0\sqrt{\pi})^3} e^{-(v^2/v_0^2)} \quad (18)$$

with  $v_0 = 220\text{Km/s}$ . This velocity distribution does not go to zero at some finite velocity. So on this one imposes by hand an upper velocity bound (escape velocity),  $v_{esc} = 2.84v_0$ . One then must transform this distribution to the lab frame,  $v \rightarrow v + v_0$ , since  $v_0$  is also the velocity of the sun around the center of the galaxy. We will not be concerned here with the motion of the Earth around the sun, i.e., the modulation effect [28]

Folding both the numerator and denominator of Eq. (2) with the LSP velocity distribution, after multiplying each with the LSP flux

$$\frac{\rho(0)}{m_\chi} \frac{m}{Am_p} v$$

we obtain the differential ratio  $\frac{1}{R} \frac{dR_e}{dT}$ , with  $R_e$  the rate for the ionization, on the form

$$\begin{aligned} \frac{1}{R} \frac{dR_e}{dT} &= \frac{d\sigma(T)}{\sigma_{nrec}} = \sum_{nl} p_{nl} |\tilde{\phi}_{nl}(\sqrt{2m_e T})|^2 m_e \sqrt{2m_e T} \\ &\times \frac{\int_{v_{min}}^{v_{max}} N v^2 e^{-v^2/v_0^2} \sinh(2v/v_0) dv}{\int_{v_{min}}^{v_{max}} D v^2 e^{-v^2/v_0^2} \sinh(2v/v_0) dv} dT \end{aligned} \quad (19)$$

where the numerator factor  $N$  and the denominator factor  $D$  are given respectively

$$N = \frac{2}{a_1^2} \int_{a_2}^{a_3} q_b F^2(q_b) dq_b, \quad q_b = qb \quad (20)$$

$$D = \frac{2}{a_1^2} \int_0^{a_1} q_b F^2(q_b) dq_b, \quad q_b = qb \quad (21)$$

where

$$a_1 = \frac{2\mu_r \nu b}{\hbar c^2}, \quad a_2 = \frac{\mu_r \nu b}{\hbar c^2} \xi_L, \quad a_3 = \frac{\mu_r \nu b}{\hbar c^2} (1 + \sqrt{1 - \xi_L}) \quad (22)$$

and  $b$  is the width of the harmonic oscillator potential.

In Eq. (19)  $v_{max}$  is the escape velocity, while  $v_{min}$  is given by Eq. (5), i.e.

$$v_{min} = \sqrt{\frac{2(T - \epsilon_{nl})}{\mu_r}} \quad (23)$$

while for the nuclear recoils:

$$v'_{min} = \frac{\sqrt{2Am_p Q_{th}}}{2\mu_r} \quad (24)$$

It is clear that the fraction in Eq. (19) is a decreasing function of the outgoing electron energy  $T$  as well as the binding energy  $-\epsilon_{nl}$  of the initial electrons. For  $T$  in the sub-keV region, where the differential rate becomes sizable,  $v_{min}$  is determined essentially by the energy of the bound electron. This restriction on the velocity distribution is a source of suppression of the rate associated with the inner shell electrons in the case of heavy targets, in particular, the 1s electrons. In fact for Xe for  $T \cong 0$  this fraction reaches the maximum values of 0.13, 0.75, 0.76 and 0.95 for 1s, 2s, 2p and 3s respectively. For lighter systems this kinematical suppression is not important even for the 1s orbits. Further suppression comes, of course, from the behavior of the bound electron wave function.

### 3 Results and Discussion

We begin our discussion by focusing on the differential rate. It is useful to divide it by the total nuclear recoil rate, i.e.  $\frac{1}{R} \frac{dR_e}{dT}$ , in order to make our results independent of the details of the SUSY parameter space and related uncertainties. From previous work [25] on  $^{20}\text{Ne}$  with hydrogenic wave functions we know that the differential rate sharply picks at low electron energies. This result is confirmed by our present calculation employing realistic electron wave functions. This is exhibited by considering three different atoms

( $^{40}\text{Ar}$ ,  $^{76}\text{Ge}$  and  $^{132}\text{Xe}$ ) for the typical LSP mass  $m_\chi = 100$  GeV (see Figs. 1-5). If we then integrate the differential rate  $\frac{1}{R} \frac{dR_e}{dT}$  with respect to the electron kinetic energy  $T$ , we obtain the relevant event rate ratio  $\frac{R_e}{R}$ . The thus obtained results for a number of nuclei are shown in Fig. 3a. They are presented as a function of the threshold energy for electron detection  $E_{th}$  for LSP mass  $m_\chi = 100$  GeV. We also present them as functions of the LSP mass  $m_\chi$ , for  $E_{th} = 0.2$  keV (Fig. 3b). We clearly see that the results are very sensitive to the threshold energy. It is also clear that the heavier targets are favored. It is encouraging that branching ratios per electron of 10% are possible, if one can reach threshold energies as low as 200 eV, which is feasible for gas targets [25]. It should be mentioned that in obtaining these results we assumed threshold effects for the ionization electrons, but not for the nuclear recoils. The nuclear recoil rate is less sensitive to the threshold in the sub-keV region.

As is well known the recoil experiments suffer from the effect of quenching. The idea of quenching is introduced, since, for low energy recoils, only a fraction of the total deposited energy goes into ionization. The ratio of the amount of ionization induced in the gas due to nuclear recoil to the amount of ionization induced by an electron of the same kinetic energy is referred to as a quenching factor  $Qu_{fac}(Q)$ . This factor depends mainly on the detector material, the recoiling energy  $Q$  as well as the process considered [41]. In our estimate of  $Qu_{fac}(Q)$  we assumed a quenching factor of the following empirical form motivated by the Lidhard theory [41]-[42]:

$$Qu_{fac}(Q) = r_1 \left[ \frac{Q}{1keV} \right]^{r_2}, \quad r_1 \simeq 0.256 \quad , \quad r_2 \simeq 0.153, \quad (25)$$

where  $Q$  is the nuclear recoil energy. The quenching factor  $Qu_{fac}(Q)$  is shown in Fig. 4. Since, as we have mentioned, we expect a threshold energy of 10 keV and the quenching factor becomes  $\approx 0.3$  above this energy, the branching ratio will increase by another factor of three, if the quenching is taken into account.

The number of electron events divided by the nuclear recoil events is obtained by multiplying the above branching ratios with the atomic number  $Z$ . This enhancement makes it possible to detect electron events not only with TPC detectors but nuclear double beta decay detectors [43], sensitive to detection of low energy electrons  $\sim 1keV$ .

With this number of events one wonders, if one can detect X rays formed after the inner shell electron hole, created by the LSP- nucleus collision, is

filled by one of the outer electrons, with or without coincidence measurement of the outgoing particles (electrons and/or recoiling nuclei). In fact we find that some inner shell orbits, in particular 2p and 3d, can make a sizable contribution. It thus seems that such X rays can be exploited. Discussion of this phenomenon as well as the background of the Auger electrons involving the inner shell electrons [25] will be discussed in detail in a separate publication. So far, the ratio of the electron rate to the recoil rate is normalized to one electron per atom. In practice, the total electron rate for given detector mass is obtained by multiplying the above rate per electron by the atomic number  $Z$ . Then the ratio of the total electron rate to the recoil rate is plotted as a function of the threshold energy in Figs 5, 6. Here in addition a quenching factor of  $\approx 0.3$  is used for the nuclear recoil. The thus obtained ratio is very impressive, even at an electron threshold higher than 0.5 keV. Thus it is interesting to search for electrons with the high-sensitivity low-threshold detectors such as those used for double beta decays discussed in recent review papers [43]

## 4 Concluding Remarks

We have explored a novel process for the direct detection of dark matter, that is by exclusive observation of the low energy ionization electrons produced during the LSP-nucleus collision. We have applied our formalism in a variety of atoms employing realistic electron wave functions and nuclear form factors. We have focused in noble gases, since we expect that low energy electrons can better be detected by gaseous TPC detectors. Our results, however, can be applied, if necessary, in other targets, e.g. those employed in neutrinoless double beta decay, since we find that the details of the electronic structure are not very important.

To minimize the uncertainties arising from SUSY and to make the presentation as simple as possible, we have calculated the ratio of the rate associated with this process divided by the rate for the standard nuclear recoils. We find that this ratio per electron slightly increases with the atomic number. It depends appreciably of the electron and the nuclear recoil energy cut offs. It is quite important to make the electron detection energy cut off as low as possible. Branching ratios (per electron) of about 10% can realistically be expected for reasonable choices of these threshold energies. Thus the ratio of the number of electron events per atom divided by the number of recoils,

obtained from the previous ratio after multiplication with the atomic number  $Z$ , can even become larger than unity. Thus, since the ionization electrons extend to the keV region, their contribution has to be taken into account in the the standard nuclear recoil experiments as well.

As it has been previously shown [25] the background problem are no worse than those appearing in the standard recoil experiments. They can be further reduced by coincidence experiments, by measuring the ionization electrons in coincidence nuclear recoils. Finally it should noted that the inner shell electron holes, created during the LSP-nuclear collision, can be filled by emitting X rays and/or Auger electrons. Such issues, which are of experimental interest, will be discussed in detail elsewhere.

In view of the above considerations it is realistic to search for WIMPs by measuring ionization electrons.

## 5 Acknowledgments

The first author (Ch.C. M.) acknowledges support by the Greek State Grants Foundation (IKY) under contract (515/2005) and would like to thank Prof. G.J. Gounaris for useful discussions concerning the atomic wave functions and the electron binding energies. The second author (J.D. V.) is indebted to the Greek Scholarship Foundation (IKYDA) for support and to Professor Faessler for his hospitality in Tuebingen. The other author ( H. E) thanks the Institute for Nuclear Theory at the University of Washington and the Department of Energy for partial support during the completion of this work. Finally all authors would like to thank Prof. C.F. Bunge for kindly providing the data for the atomic wave functions.

## References

- [1] S. Hanary *et al.*, *Astrophys. J.* **545**, L5 (2000); J.H.P Wu *et al.*, *Phys. Rev. Lett.* **87**, 251303 (2001); M.G. Santos *et al.*, *Phys. Rev. Lett.* **88**, 241302 (2002).
- [2] P.D. Mauskopf *et al.*, *Astrophys. J.* **536**, L59 (20002); S. Mosi *et al.*, *Prog. Nuc.Part. Phys.* **48**, 243 (2002); S.B. Ruhl *et al.*, *Astrophys. J.* **599**, 786 (2003) and references therein.

- [3] N.W. Halverson *et al.*, *Astrophys. J.* **568**, 38 (2002); L.S. Sievers *et al.*, astro-ph/0205287 and references therein.
- [4] G.F. Smoot *et al.*, (COBE data), *Astrophys. J.* **396**, (1992) L1.
- [5] D.N. Spergel *et al.*, *Astrophys.J.Suppl.* **148** (2003) 175; astro-ph/0302209.
- [6] M. Tegmark *et al.*, *Phys.Rev. D* **69** (2004) 103501; astro-ph/0310723.
- [7] A.H. Jaffe *et al.*, *Phys. Rev. Lett.* **86**, 3475 (2001).
- [8] D.P. Bennett *et al.*, (MACHO collaboration), A binary lensing event toward the LMC: Observations and Dark Matter Implications, Proc. 5th Annual Maryland Conference, edited by S. Holt (1995); C. Alcock *et al.*, (MACHO collaboration), *Phys. Rev. Lett.* **74**, 2967 (1995).
- [9] R. Bernabei *et al.*, INFN/AE-98/34, (1998); R. Bernabei *et al.*, *Phys. Lett. B* **389**, 757 (1996).
- [10] R. Bernabei *et al.*, *Phys. Lett. B* **424**, 195 (1998); *B* **450**, 448 (1999).
- [11] A. Benoit *et al.*, [EDELWEISS collaboration], *Phys. Lett. B* **545**, 43 (2002); V. Sanglar, [EDELWEISS collaboration], arXiv:astro-ph/0306233.
- [12] D.S. Akerib *et al.*, [CDMS collaboration], *Phys. Rev D* **68**, 082002 (2003); arXiv:astro-ph/0405033.
- [13] For a review see: G. Jungman, M. Kamionkowski and K. Griest, *Phys. Rep.* **267**, 195 (1996).
- [14] M.W. Goodman and E. Witten, *Phys. Rev. D* **31**, 3059 (1985).
- [15] K. Griest, *Phys. Rev. Lett.* **61**, 666 (1988).
- [16] J. Ellis, and R.A. Flores, *Phys. Lett. B* **263**, 259 (1991); *Phys. Lett. B* **300**, 175 (1993); *Nucl. Phys. B* **400**, 25 (1993).
- [17] J. Ellis and L. Roszkowski, *Phys. Lett. B* **283**, 252 (1992).

- [18] For more references see e.g. our previous report: J.D. Vergados, Supersymmetric Dark Matter Detection- The Directional Rate and the Modulation Effect, hep-ph/0010151.
- [19] M.E.Gómez and J.D. Vergados, *Phys. Lett. B* **512** , 252 (2001); hep-ph/0012020. M.E. Gómez, G. Lazarides and C. Pallis, Phys. Rev. D **61**, 123512 (2000) and *Phys. Lett. B* **487**, 313 (2000).
- [20] M.E. Gómez and J.D. Vergados, hep-ph/0105115.
- [21] A. Bottino *et al.*, Phys. Lett B **402**, 113 (1997); R. Arnowitt. and P. Nath, Phys. Rev. Lett. **74**, 4952 (1995); Phys. Rev. D **54**, 2394 (1996); hep-ph/9902237; V.A. Bednyakov, H.V. Klapdor-Kleingrothaus and S.G. Kovalenko, Phys. Lett. B **329**, 5 (1994).
- [22] U. Chattopadhyay A. Corsetti and P. Nath, Phys. Rev. D **68**, 035005 (2003).
- [23] U. Chattopadhyay and D.P. Roy, Phys. Rev D **68**, 033010 (2003); hep-ph/0304108.
- [24] B. Murakami and J.D. Wells, Phys. Rev. D **64** (2001) 015001; hep-ph/0011082.
- [25] J.D. Vergados and H. Ejiri, Phys. Lett. B **606** (2005) 305; hep-ph/0401151.
- [26] D.N. Spergel, Phys. Rev. **37**, (1988) 1353; J.D. Lewin and P.F. Smith, Astropart. Phys. **6**, (1996) 87; C.J. Copi, J. Heo and L.M. Krauss, Phys. Lett. **461** B, 43 (1999); D. Akimov *et al*, Phys. Lett. **525** B, 245 (2002); B. Morgan, A.M. Green and N. Spooner astro-ph/0408047.
- [27] D.P. Snowden-Ifft, C.C. Martoff and J.M. Burwell, Phys. Rev. D **61**, 1 (2000); M. Robinson *et al.*, Nucl. Inst. Meth. A **511**, 347 (2003); K.N. Buckland, M.J. Lehner and G.E. Masek, In Proc. 3rd Int. Conf. on Dark Matter in Astro and Part. Phys. (Dark2000), Ed. V.N. Klapdor-Kleingrothaus, Springer Verlag (2002).
- [28] J.D. Vergados, Phys. Rev. D **67** (2003) 103003; *ibid* **58** (1998) 10301-1; J.D. Vergados, J. Phys. G: Nucl. Part. Phys. **30**, 1127 (2004).

- [29] M.J. Carson *et al.*, *Astropart. Phys.* **21** (2004) 667; See also: M.J. Carson *et al.*, hep-exp/0503017; B. Morgan, A.M. Green and N.J.C. Spooner, astro-ph/0408047.
- [30] J.D. Vergados, P. Quentin and D. Strottman, hep-ph/0310365 (to be published).
- [31] H. Ejiri, K. Fushimi and H. Ohsumi, *Phys. Lett. B* **317**, 14 (1993).
- [32] Y. Giomataris and J.D. Vergados, *Nucl.Instr. Meth. A* **530**, 330 (2004).
- [33] The NOSTOS experiment and new trends in rare event detection, I. Giomataris et al., hep-ex/0502033, submitted to the SIENA2004 International Conference (2005).
- [34] Y. Giomataris, P. Rebourgeard, J.P. Robert, Georges Charpak, *Nucl. Instrum. Meth. A* **376** (1996) 29.
- [35] J.D. Vergados, *J. Phys. G: Nucl. Part. Phys.* **22** (1996) 253.
- [36] J. Hisano, M. Nagai, M.M. Nojiri and M. Senami, hep-ph/0504068.
- [37] P.C. Divari, T.S. Kosmas, J.D. Vergados and L.D. Skouras, *Phys. Rev. C* **61**, 054612 (2000).
- [38] C.F. Bunge, J.A. Barrientos, and A.V. Bunge, *At. Data Nucl. Data Tables* **53**, 113 (1993).
- [39] G.J. Gounaris, E.A. Paschos, and P.I. Porfyriadis, *Phys. Rev. D* **70**, 113008, (2004).
- [40] <http://www.webelements.com/webelements/>;  
<http://www.chembio.uoguelph.ca/educmat/atomdata/bindener/elecbind.htm>
- [41] E. Simon *et al.*, *Nucl. Instr. Meth. A* 507 (2003) 643; astro-ph/0212491.
- [42] J. Lidhart *et al.*, *Mat. Phys. Medd. Dan. Vid. Selsk.* 33 (10) (1963) 1.
- [43] See e.g.:  
F. Avignone, *Proc. Neutrino Conference,  $\nu$  2004*, (2004);  
S.R. Elliot and J. Engel, *J. Phys. G30* (2004) R183;  
H. Ejiri, *J. Phys. Soc. Japan*, Invited review paper, Aug. 2005;



C. Aalseth *et al*, Neutrinoless double beta decay and direct searches for neutrino mass, hep-ph/0412300; and references therein.

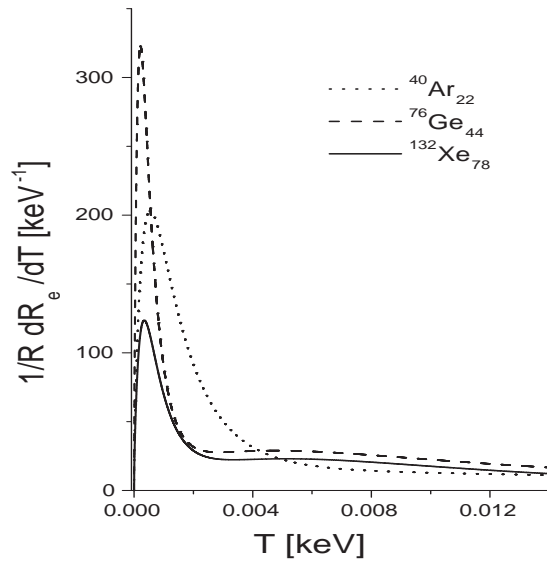


Figure 1: The differential rate for ionization electrons, divided by the total rate associated with the nuclear recoils, as a function of the electron energy  $T$  (in keV) for various atoms. The results exhibited were obtained for a typical LSP mass  $m_\chi = 100$  GeV by including a nuclear form factor, but without recoil threshold effects.

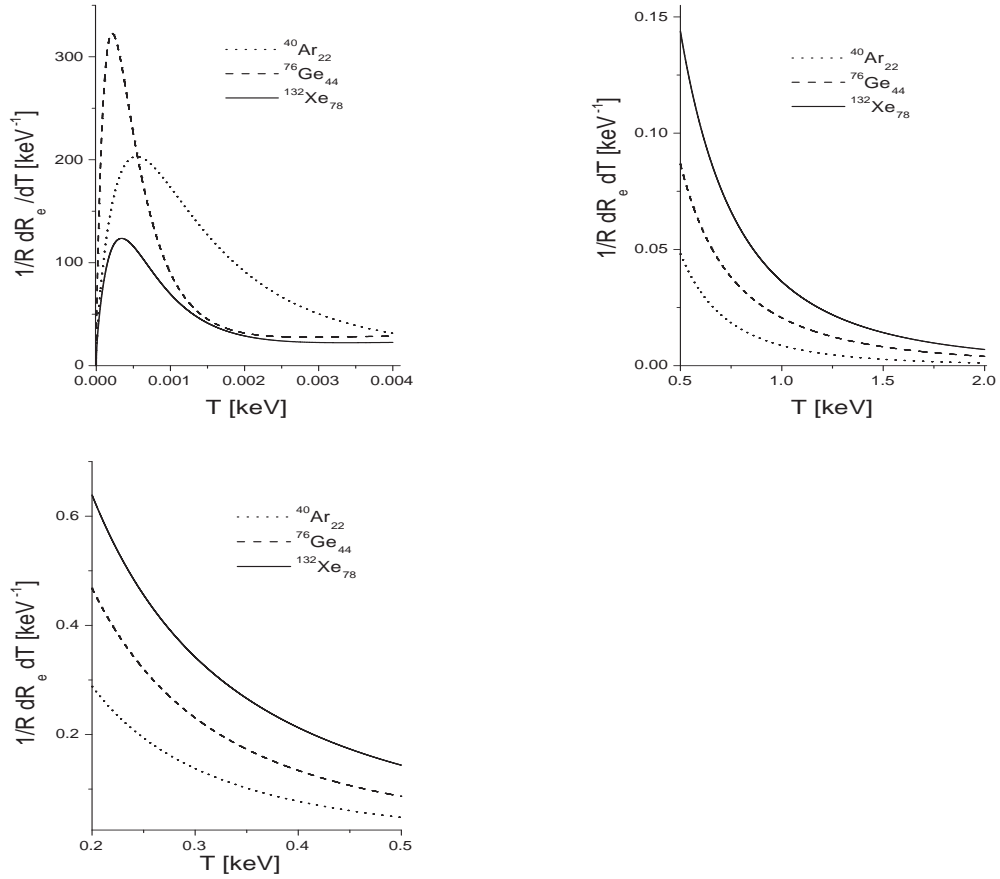


Figure 2: The same as in Fig. 1 except that we have now separated the plot in various energy intervals, so that the energy dependence at higher energies becomes visible.

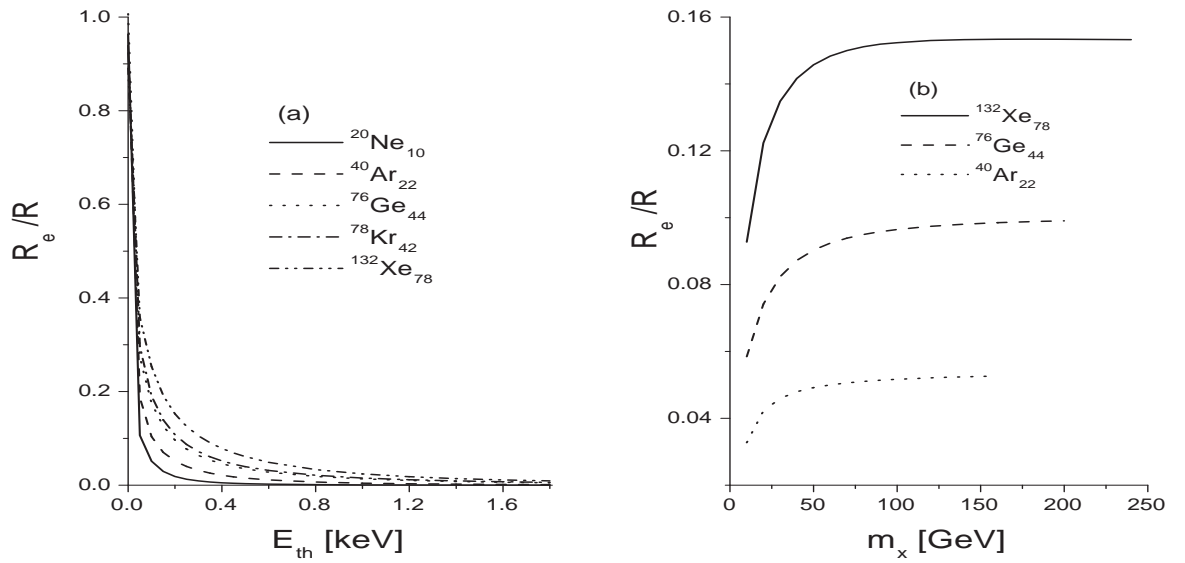


Figure 3: (a) The total ionization rate per electron divided by the standard nuclear recoil rate as a function of the electron threshold energy. The results exhibited were obtained for a typical LSP mass  $m_\chi = 100$  GeV by including a nuclear form factor, but no threshold effects on recoils. (b) The same quantity plotted as a function of the mass  $m_\chi$  of the LSP. The results were obtained for a threshold energy  $E_{th} = 0.2$  keV

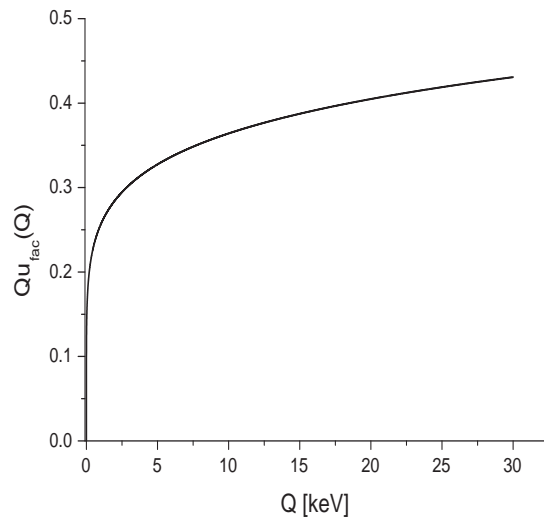


Figure 4: The quenching factor  $Qu_{fac}(Q)$  as a function of the recoil energy  $Q$  in  $keV$ .

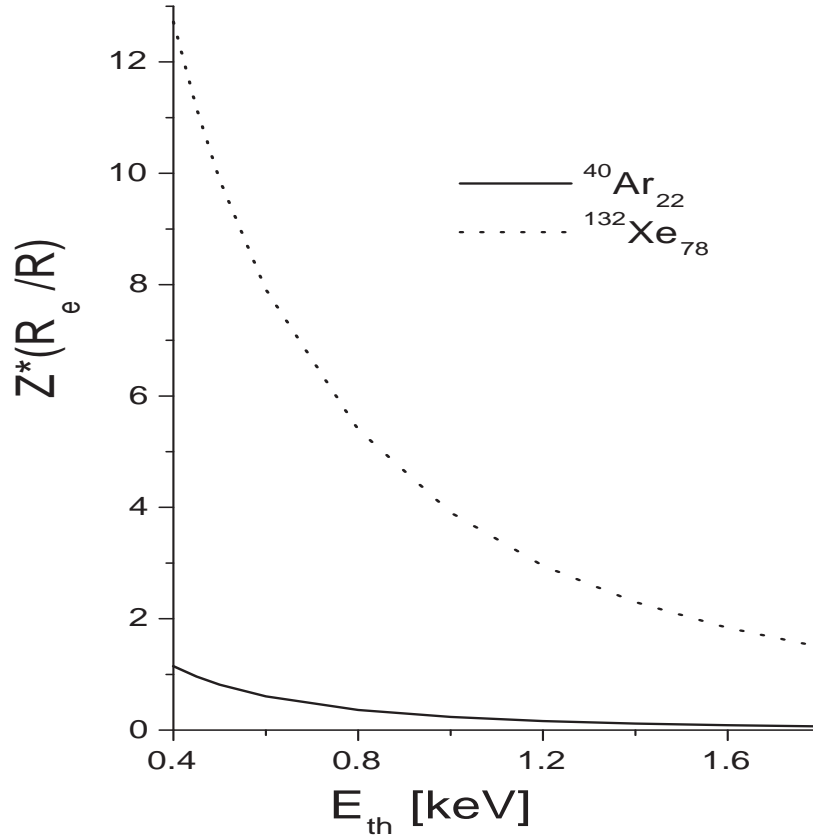


Figure 5: The same as in Fig. 3a except that now the ionization rate  $R_e$  per electron is multiplied by the atomic number  $Z$  to obtain the rate per atom. In other words we plot the relative ionization rate  $ZR_e$  per atom with respect to the nuclear recoil rate, i.e.  $r = Z\frac{R_e}{R}$ . The quenching factor of about 1/3 has also been included in the denominator. More precisely we use  $(1/3)R$  for the denominator (standard recoil) to incorporate the reduction of the recoil rate with a typical threshold and quenching factor (see Fig. 4).

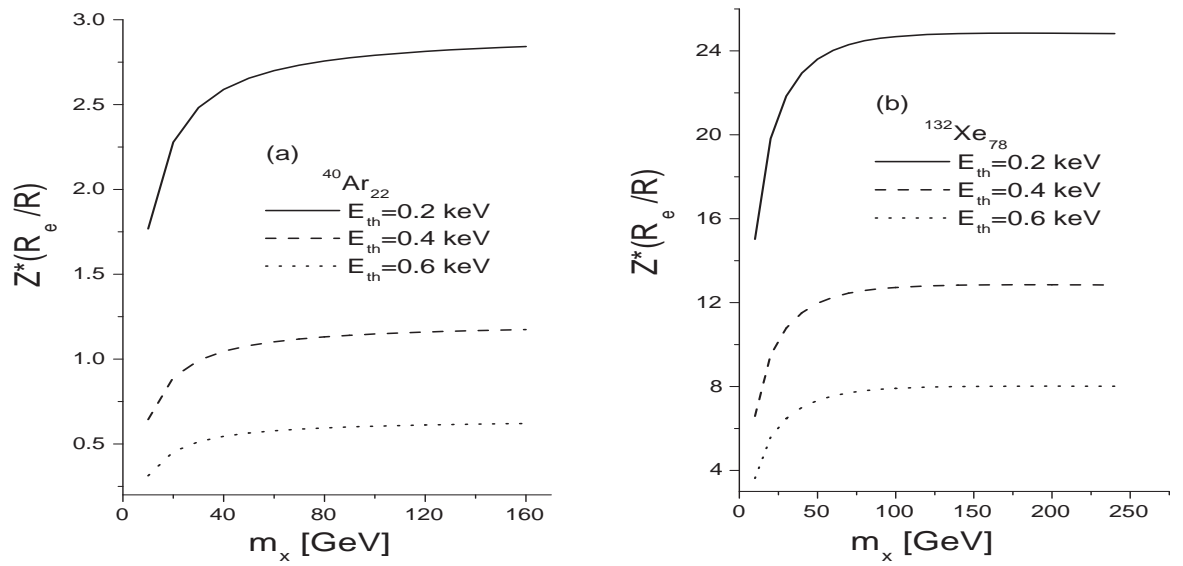


Figure 6: The same as in Fig. 3b except that now the electron ionization rate per electron has been multiplied by the atomic number  $Z$  (the relative event rate per atom is  $r = Z \frac{R_e}{R}$ ). The quenching factor of about  $1/3$  has also been included in the denominator (standard nuclear recoil).